J. R. Culham
Associate Professor and Director
Mem. ASME

M. M. Yovanovich
Distinguished Professor Emeritus
Fellow ASME

P. Teertstra
Research Associate

Microelectronics Heat Transfer Laboratory,
Department of Mechanical Engineering,
University of Waterloo,
Waterloo, ON, Canada

C.-S. Wang
Advanced Thermal Solutions, Newton, MA

G. Refai-Ahmed
Solinet Systems, Ottawa, ON, Canada
Mem. ASME

Ra-Min Tain
Nortel Metworks, Kanata, ON, Canada

Simplified Analytical Models for Forced Convection Heat Transfer From Cuboids of Arbitrary Shape

Three analytical models are presented for determining laminar, forced convection heat transfer from isothermal cuboids. The models can be used over a range of Reynolds number, including at the diffusive limit where the Reynolds number goes to zero, and for a range of cuboid aspect ratios from a cube to a flat plate. The models provide a simple, convenient method for calculating an average Nusselt number based on cuboid dimensions, thermophysical properties and the approach velocity. Both the cuboid and the equivalent flat plate models are strongly dependent upon the flow path length which is bounded between two easily calculated limits. In comparisons with numerical simulations, the models are shown to be within ±6 percent over the range of $0 \leqslant Re_{\sqrt{A}} \leqslant 5000$ *and aspect ratios between 0 and 1.* [DOI: 10.1115/1.1347993]

Introduction

Numerous practical applications in the design of electronics and telecommunications equipment depend upon low-velocity, laminar flow as a mechanism for dissipating heat. A diverse range of applications are typically encountered, including heat transfer from printed circuit boards with low profile chip-on-board packages, cooling of electronic packages, transformers, heat sinks, thermal spreaders plus many other complex components that require some means of forced convection cooling to maintain safe operating temperature limits.

Several researchers have investigated forced convection from isothermal axisymmetric bodies, such as spheroids (Beg [1]), cylinders (Refai-Ahmed and Yovanovich [2]) and disks (Wedekind and Kobus [3] using a variety of predictive methods as reviewed in Yovanovich [4]. However, the number of studies for steady laminar forced convection heat transfer from isothermal cuboids is very limited, with most research restricted to experimental studies (Igarashi [5,6]) leading to empirical correlations or detailed numerical procedures (Wong and Chen [7]). Few simple, analytical procedures are available because of the perceived difficulty in modeling the vertical faces of the cuboid, perpendicular to the flow direction.

The principal objective of this paper is to present several, analytical models for calculating the overall rate of heat transfer from isothermal cuboids of varying aspect ratios. Models will be simple functions of easily attainable information such as cuboid dimensions, flow conditions and thermophysical properties.

The models presented are intended for isothermal boundary conditions but it is interesting to note that in spherical bodies the overall rate of heat transfer is identical for both isothermal and isoflux boundary conditions. While the rate of heat transfer will be different for isothermal and isoflux conditions as the aspect ratio is varied, the change is relatively small and in most instances the models can be used for nonisothermal conditions.

Contributed by the Electrical and Electronic Packaging Division for publication in the JOURNAL OF ELECTRONIC PACKAGING. Manuscript received at ASME Headquarters October 13, 2000. Associate Editor: R. Schmidt.

Modeling Procedure

The overall rate of heat transfer from an isothermal, convex body is a function of several fundamental modes of heat transfer including diffusion, convection and radiation. If we assume the radiative component to be relatively small, an overall Nusselt number based on a general characteristic length, $\mathcal{L}$ can be defined as a function of two limiting asymptotes, as shown in Eq. (1).

$$\mathrm{Nu}_{\mathcal{L}} = [(S^*)^n + (\mathrm{Nu}_{bl})^n]^{1/n} \tag{1}$$

The first asymptote is based on the diffusion or conduction of heat as the flow velocity approaches zero, while the second asymptotic limit is based on laminar boundary layer flow for flow velocities greater than zero. Yovanovich [8] (forced convection, spheroids), Yovanovich and Vanoverbeke [4] (mixed convection, spheroids), Refai-Ahmed and Yovanovich [2] (forced convection, circular and square cylinders and toroids), Wang et al. [9] (natural convection, heat sinks), and Lee et al. [10] (natural convection, general body shapes) have all used this approach to obtain analytical models that are applicable over a wide range of flow conditions.

The procedure of combining limiting asymptotic solutions was first employed by Churchill and Usagi [11]. The method presented by Churchill and Usagi takes two analytical solutions that are known to be ''exact'' at predefined limits and provides a means of transitioning smoothly between these two limits, thereby obtaining a comprehensive analytical procedure that is a function of a single unknown constant, *n*, that is typically referred to as the blending parameter. Equation (1) satisfies exactly both limiting asymptotic solutions, however in the transition between the two limits the blending parameter, *n* can be used to minimize differences between the model and known experimental or numerical data. Typical values for the blending parameter can vary between unity (superposition) and real numbers in the range of 1–5. The higher the value of the blending parameter the greater the tendency for the model to map the asymptotic solutions near the intersection point of the two limiting models.

Based on comparisons between numerical validation data and

the models presented herein, a value of $n=1.3$ has been found to provide the best agreement over the full range of flow conditions and geometric constraints.

Diffusive Limit. A general expression for calculating the conduction shape factor (diffusive limit) of a cuboid with dimensions $L_1\times L_2\times L_3$ can be determined based on procedures developed by Yovanovich (Rohsenow et al. [12]). The procedure involves first calculating the shape factor of an infinitely thin rectangular plate on the face of the cuboid with aspect ratio nearest to unity. This entails using the mean value of the shape factors calculated for circumscribed and inscribed circles, as shown in Fig. 1. If we assume face L_1-L_2 has as an aspect ratio nearest to unity, two formulations are available for calculating the conduction shape factor based on the range of the aspect ratio, L_1/L_2, where $L_1\geqslant L_2$.

$$[S^*_{\sqrt{A}}]_{\text{plate}}=\frac{\sqrt{\frac{2}{\pi}}\left(1+\sqrt{\frac{L_1}{L_2}}\right)^2}{\sqrt{\frac{L_1}{L_2}}},\quad 1.0\leqslant\frac{L_1}{L_2}\leqslant 5.0 \tag{2}$$

$$=\frac{2\sqrt{2\pi}\sqrt{\frac{L_1}{L_2}}}{\ln\left(4\frac{L_1}{L_2}\right)},\quad 5.0\leqslant\frac{L_1}{L_2}<\infty \tag{3}$$

The shape factor for the infinitely-thin rectangular plate, as given in Eqs. (2) and (3) is then corrected to account for the third dimension of the cuboid using a procedure presented by Yovanovich (Rohsenow et al. [12]) based on the right circular cylinder model of Smythe [13,14], such that

$$S^*_{\sqrt{A}}=|S^*_{\sqrt{A}}|_{\text{plate}}\cdot\left[\frac{1+0.8688(L_3/D_{GM})^{0.76}}{\sqrt{1+2L_3/D_{GM}}}\right] \tag{4}$$

where D_{GM} is the mean diameter of the inscribed and circumscribed circles which is then extended along the L_3 axis to form a circular cylinder as shown in Fig. 1.

$$D_{GM}=\sqrt{\frac{2}{\pi}(L_1+L_2)\cdot\sqrt{L_1^2+L_2^2}} \tag{5}$$

Boundary Layer Forced Convection. Three unique approaches to modeling forced convection heat transfer from isothermal cuboids of arbitrary aspect ratio will be presented. The models range in their level of simplicity and in their ability to accurately predict heat transfer over the full range of aspect ratios.

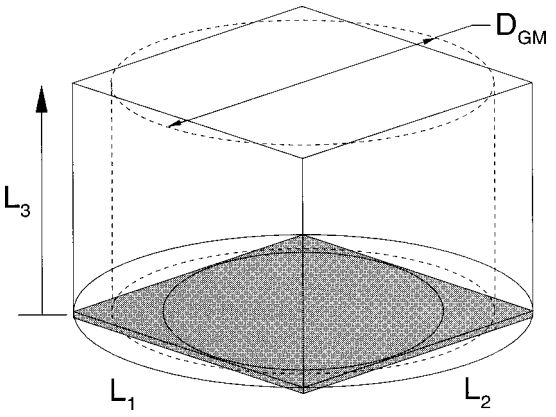

Fig. 1 Procedure for calculating the conduction shape factor of a cuboid

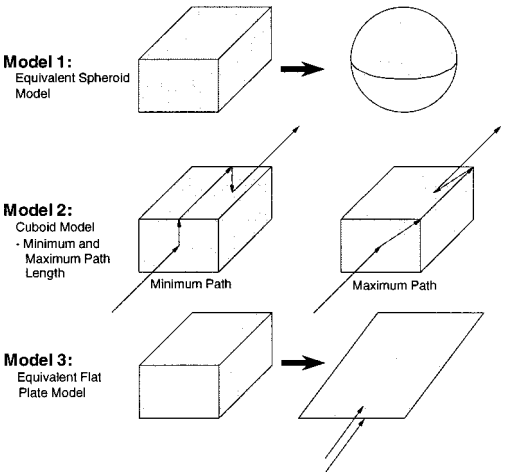

Fig. 2 Modeling procedures for boundary layer flow

The procedures used to model forced convection from cuboids are shown schematically in Fig. 2, with the three models identified as:

1 Equivalent Spheroid Model: A spheroid of equivalent surface area to a cuboid is modeled based on formulations presented by Yovanovich [8].

2 Cuboid Model: A cuboid model is presented based on boundary flow using a flow length established between the stagnation points at the leading and trailing surfaces of the cuboid.

3 Equivalent Flat Plate Model: A flat plate of equivalent surface area to a cuboid is modeled based on boundary layer formulations for an isothermal plate where the flow length is established based on the geometry of the cuboid.

Equivalent Spheroid Model. Given a cuboid with dimensions $H\times L\times W$, as shown in Fig. 3, an equivalent spheroid can be obtained where the total surface area is preserved. Yovanovich [8] presents a correlation equation for steady, axisymmetric, laminar forced convection from isothermal spheroids in the Reynolds number range: $0\leqslant \text{Re}_{\mathcal{L}}\leqslant 10^5$, where the characteristic length $\mathcal{L}$ is the square root of the wetted surface area of the body. The Yovanovich correlation can be used for a range of aspect ratios, including oblate spheroids ($AR<1$), spheres ($AR=1$) and prolate spheroids ($AR>1$). Yovanovich combines two range specific equations developed by Yuge [15] using the blending procedure to produce a single correlation equation for Nusselt number which is accurate to within ± 5 percent.

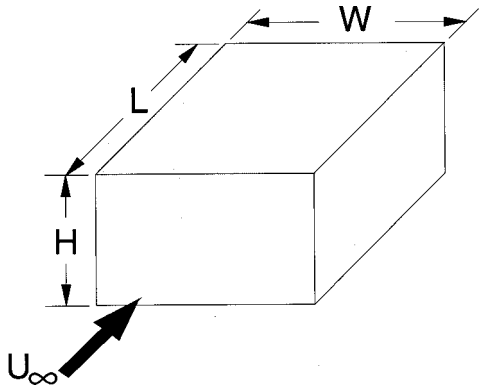

Fig. 3 Cuboid dimensions

$$\mathrm{Nu}_{\sqrt{A}} = S^*_{\sqrt{A}} + [0.15(P/\sqrt{A})^{1/2}\,\mathrm{Re}^{1/2}_{\sqrt{A}} + 0.27(P/\sqrt{A})^{0.4336}\,\mathrm{Re}^{0.5664}_{\sqrt{A}}]\mathrm{Pr}^{1/3} \quad (6)$$

where P is the maximum perimeter formed by the profile of the body in the flow direction and A is the total surface area of the body.

Although Eq. (6) was originally developed for laminar, forced convection from spheroids with aspect ratios, $0 \leqslant AR \leqslant 5$, the same equation can be used for cuboids where the $P/\sqrt{A}$ is based on the geometry of the cuboid and the conduction shape factor can be calculated based on Eqs. (2)–(5).

Cuboid Model. A local Nusselt number, based on a flow length x, can be written for laminar, boundary layer flow over an isothermal body of arbitrary shape such that

$$\mathrm{Nu}_x = \mathrm{Re}^{1/2}_x F(\mathrm{Pr}) \quad (7)$$

Yovanovich et al. [16], have demonstrated that using the transient solution for heat diffusion from a homogeneous half space, an analogous solution can be obtained for boundary layer flow with $\mathrm{Pr} \rightarrow \infty$ such that

$$F(\mathrm{Pr}) = \frac{1}{\sqrt{\pi \cdot C}}\,\mathrm{Pr}^{1/3} \quad (8)$$

Combining Eqs. (7) and (8) yields

$$\mathrm{Nu}_x = \frac{1}{\sqrt{\pi}} \frac{x}{\sqrt{\dfrac{\alpha C x \mathrm{Pr}^{1/3}}{U_\infty}}} \quad (9)$$

where an effective residence time, t_e can be introduced with the path length, L_p, substituted for x.

$$t_e = \frac{L_p (C \cdot \mathrm{Pr}^{1/3})}{U_\infty} \quad (10)$$

Combining Eqs. (9) and (10) leads to a local Nusselt number defined as

$$\mathrm{Nu}_x = \frac{1}{\sqrt{\pi}} \frac{x}{\sqrt{\alpha t_e}} \quad (11)$$

and the average Nusselt number based on an arbitrary characteristic length, $\mathcal{L}$, is written as

$$\mathrm{Nu}_{\mathcal{L}} = \frac{2}{\sqrt{\pi}} \frac{\mathcal{L}}{\sqrt{\alpha t_e}} \quad (12)$$

or in terms of dimensionless parameters, $\mathrm{Re}_{\mathcal{L}}$ and Pr as

$$\mathrm{Nu}_{\mathcal{L}} = \frac{2}{\sqrt{\pi}} \frac{1}{\sqrt{\dfrac{L_p \cdot C}{\mathrm{Re}_{\mathcal{L}} \mathrm{Pr}^{2/3} \mathcal{L}}}} \quad (13)$$

Lee et al. [10] demonstrated that the square root of the surface area of a body is a superior choice as the characteristic length. In the case of a cuboid the characteristic length is

$$\mathcal{L} = \sqrt{2(H \cdot L + H \cdot W + L \cdot W)} \quad (14)$$

The length of the flow path, characterized as the distance between the stagnation points on the front and rear surfaces of a body, is bounded between two extremes defined as the minimum and maximum path lengths. As shown in Fig. 4, the minimum and maximum path lengths for a cuboid are given as

$$L_{p_{\min}} = H + L \quad (15)$$

$$L_{p_{\max}} = L + \sqrt{W^2 + H^2} \quad (16)$$

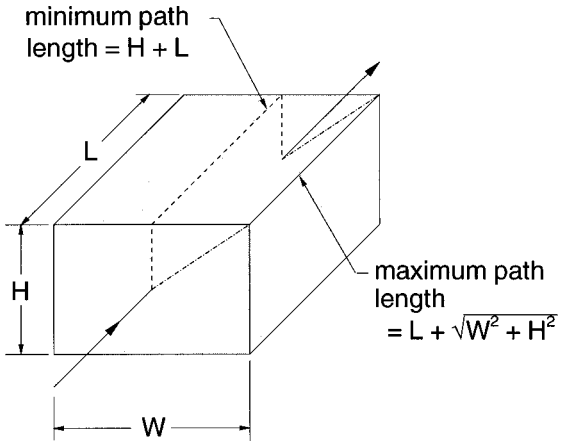

Fig. 4 Shortest and longest path

The choice of the most effective value of path length is not clearly defined based solely on analysis and can be any value between and inclusive of $L_{p\,\min}$ and $L_{p\,\max}$. Numerical simulations of cuboids of various aspect ratios indicate that the minimum path length, as defined in Eq. (15), provides the best agreement with the model predictions.

If we maintain the plan profile of the cuboid as a square (i.e., $L = W$) and define an aspect ratio as $AR = H/L$, the characteristic length and the flow path length can be defined as

$$\mathcal{L} = L \cdot \sqrt{2(AR+1)} \quad (17)$$

$$L_p = L \cdot (AR+1) \quad (18)$$

which combined with Eq. (13) gives

$$\mathrm{Nu}_{\sqrt{A}} = \frac{2}{\sqrt{\pi}} \frac{1}{\sqrt{\dfrac{(AR+1)\cdot C}{\sqrt{2(AR+1)}}}} \mathrm{Re}^{1/2}_{\sqrt{A}} \mathrm{Pr}^{1/3} \quad (19)$$

The boundary layer parameter, C can be shown (Schlichting [17]) to be equivalent to

$$C = \frac{U_\infty}{u_e} \quad (20)$$

where u_e is an effective velocity based on a linearization of the laminar boundary layer momentum equation. Two methods are available for obtaining a numerical value for C. A value of $C = 2.77$ is obtained for high Prandtl numbers when the heat flux at the surface of the body is assumed to be that of the ''exact'' solution of Pohlhausen [18]. The second method which gives a value of $C = 2.13$ is based on an enthalpy heat flux balance across the thermal boundary layer for transient heat diffusion in a half space.

Table 1 shows the influence of varying C on Nusselt number for forced convection over the range of Reynolds number inves-

Table 1 Influence of *C* on the convective component of the Nusselt number

Body	C	$\mathrm{Re}_{\sqrt{A}}$ 1	10	100	1000	5000
cube	2.13	0.76	2.41	7.63	24.14	53.97
	2.5	0.70	2.23	7.05	22.28	49.82
	2.77	0.67	2.12	6.69	21.17	47.33
plate	2.13	0.82	2.59	8.20	25.94	58.00
	2.5	0.76	2.39	7.57	23.94	53.54
	2.77	0.72	2.27	7.19	22.75	50.86

Table 2 Upper and lower bounds on Nusselt number for a flat plate solution

Bound	L_{plate}	W_{plate}	Active surfaces
upper	$\frac{H\cdot L+H\cdot W+L\cdot W}{H+W}$	$2(H+W)$	1-sided
		$(H+W)$	2-sided
lower	$(L+H)$	$\frac{2(H\cdot L+H\cdot W+L\cdot W)}{L+H}$	1-sided
		$\frac{H\cdot L+H\cdot W+L\cdot W}{L+H}$	2-sided

tigated in this study. A maximum difference of 12 percent on Nusselt number is observed at $\text{Re}_{\sqrt{A}}=5000$. Using a simple average of the two extremes, i.e., $C=2.5$ results in a maximum difference of ± 6 percent on Nusselt number.

Equivalent Flat Plate Model. The average Nusselt number for forced convection boundary layer flow over an isothermal flat plate of flow length L_p is given as

$$\text{Nu}_{L_p}=C\,\text{Re}_{L_p}^{1/2}\text{Pr}^{1/3} \tag{21}$$

where Yovanovich and Teertstra [19] have demonstrated that using a linearization of the energy and momentum equations, Eq. (21) can be recast as

$$\text{Nu}_{L_p}=2F(\text{Pr})\text{Re}_{L_p}^{1/2} \tag{22}$$

with $F(\text{Pr})$ expressed as in Eq. (8) for high Prandtl number fluids (i.e., $\text{Pr}\rightarrow\infty$).

Using a value of $C=2.5$, Eq. (22) can be written as

$$\text{Nu}_{L_p}=0.714\,\text{Re}_{L_p}^{1/2}\text{Pr}^{1/3} \tag{23}$$

Changing the characteristic length, L_p to $\sqrt{A}$, to be more compatible with the other solution procedures, we obtain an average Nusselt number

$$\text{Nu}_{\sqrt{A}}=0.714\cdot\left(\frac{L_p}{\sqrt{A}}\right)^{-1/2}\cdot\text{Re}_{\sqrt{A}}^{1/2}\text{Pr}^{1/3} \tag{24}$$

Equation (24) is functionally dependent on L_p, the flow length which is bounded by two limiting values. An upper bound on the Nusselt number is obtained by simulating a plate with the same surface area as that of a cuboid and overall dimensions $L_{\text{plate}}\times W_{\text{plate}}$, where the width of the plate is equivalent to the maximum perimeter of the cuboid on a plane perpendicular to the flow direction. In effect, the leading edge surfaces formed by the planes of the cuboid are preserved and the resultant plate length is obtained by maintaining the overall surface area of the cuboid. In the case of a plate with both planar surfaces active, the width of the plate should be halved, forming a single-sided plate folded in half. The lower bound on Nusselt number can be obtained by forming a plate of equivalent surface area to a cuboid but where the length of the plate is determined based on the flow length established between the stagnation points on the leading and trailing edge of the cuboid, as given in Eq. (15).

Table 2 summarizes the plate dimensions for calculating an upper and lower bound on the Nusselt number when using the equivalent flat plate model for plates with either a single active surface i.e., one side insulated or both sides of the plate are contributing to the heat transfer.

Finite Volume Procedure. The validity of the analytical models was assessed by comparing calculations for the overall rate of heat transfer versus results obtained from simulations performed using FLOTHERM [20], a commercial, finite-volume

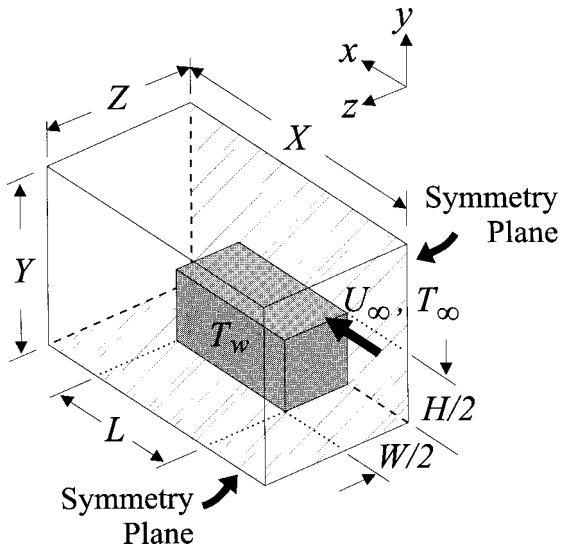

Fig. 5 Schematic of CFD solution domain

based software package. The numerical simulations were used to determine heat transfer and fluid flow in the region surrounding an isothermal cuboid, as shown in Fig. 5.

The cuboid was modeled using four isothermal, no slip planes in contact with the fluid regions for the leading, trailing, and lateral surfaces, and symmetry was applied in the streamwise direction, as shown in Fig. 5. A uniform inlet velocity U_∞ and uniform free stream temperature T_∞ were applied at the upstream domain boundary, and the downstream and lateral domain boundaries were set to atmospheric (zero) pressure, allowing heat and mass to freely exit the system. The cuboid and the ambient air temperature were set to $T_s=40°\text{C}$ and $T_\infty=20°\text{C}$, respectively, and all properties were evaluated at a film temperature of 303 K.

In each of the CFD simulations, the surface area of the cuboid was kept constant to allow comparison of the results for different aspect ratios, and equal dimensions for the length and width dimensions of the cuboid were specified. Three different cuboid configurations were examined in the numerical study, with aspect ratios $H/L=0.167$, 0.46 and 1.0. The limiting case of the flat plate, $H=0$, was also simulated to reveal solution trends for small aspect ratios.

Because of the large range of Reynolds number proposed for these simulations, $10\leqslant\text{Re}_{\sqrt{A}}\leqslant 5000$, it was anticipated that different computational domain sizes would be required, depending on the Reynolds number. For small $\text{Re}_{\sqrt{A}}$, the heat transfer is dominated by conduction, and a relatively large domain is required to simulate a conductive, full-space region. This same domain is also sufficient to model the limiting case of the diffusive limit, $\text{Re}_{\sqrt{A}}\rightarrow 0$, where the heat transfer is by conduction alone. For the small $\text{Re}_{\sqrt{A}}$ limit, the dimensions of the domain were specified as shown in Table 3, based on steady-state conduction simulation results presented by Yovanovich et al. [21]. For large Reynolds numbers, $\text{Re}_{\sqrt{A}}\geqslant 1000$, the bulk of the heat transfer from the cuboid is by convection through a thin, laminar boundary layer. The numerical simulation in this case requires many more control volumes near the body surface to accurately resolve the large temperature and

Table 3 Typical CFD solution domain dimensions

$\text{Re}_{\sqrt{A}}$	X/L	Y/L	Z/L
10	10	5	5
100	10	5	5
1000	5	1.5	1.5
5000	5	1.5	1.5

velocity gradients. In order to achieve this increased discretization while maintaining a reasonable number of control volumes, the dimensions of the solution domain were reduced as shown in Table 3. Through a convergence study it was demonstrated that the results were independent of domain size when the solution domain dimensions presented in Table 3 were used for large $Re_{\sqrt{A}}$. A schematic of the CFD solution domain used in the present simulations is presented in Fig. 5, nondimensionalized using the cuboid length in the flow direction L for the cube.

In order to demonstrate the independence of the results of the numerical simulations on the size and number of control volumes in the solution domain, a grid convergence studies was performed for an intermediate case, $H=L=W$ for $Re_{\sqrt{A}}=1000$. The size of the control volumes in the fluid region adjacent to the cuboid was reduced in a systematic manner, until the variation in the average results was less than 1 percent between subsequent discretization levels. This level of grid refinement was used for all other geometries and Reynolds numbers throughout the remainder of the study.

The total heat flow from the cuboid was determined from the numerical results using integrated values provided by the CFD software package for 4 planar control surfaces surrounding the cuboid. The net heat flow rates through each of these planar surfaces were combined to give the total heat flow rate from the cuboid to its surrounding domain.

Discussion

The effectiveness of each of the three analytical models to accurately predict the rate of heat transfer from cuboids with aspect ratios $0 \leqslant AR \leqslant 1$ is assessed through comparison with numerical predictions using a finite volume model. For each test case the surface area of the cuboid is held constant while the plan profile of the cuboid is maintained as a square ($L=W$) and the aspect ratio ($AR=H/L$) is varied between 0 (plate) and 1 (cube). The heat transfer rate is calculated for a range of Reynolds numbers between 0 and 5000, where the Reynolds number is based on an approach velocity, U_∞, a characteristic length, $\sqrt{A}$ and the kinematic viscosity calculated at 30°C. With the area of the test cuboids held constant and the properties calculated at a constant temperature, the sole factor influencing a change in the Reynolds number is the approach velocity. As the approach velocity goes to zero the heat transfer from the cuboids is based entirely on conduction effects and the resulting Nusselt number is equivalent to the conduction shape factor of the body or the diffusive limit. This conduction effect is an integral part of the Nusselt number for all tests, however its influence is minimized as convective heat transfer becomes more prominent at higher Reynolds numbers.

Yovanovich [8] has demonstrated that the spheroid model can be used with 5–10 percent confidence when compared with a variety of published spheroid correlation models over a full range of Reynolds number and aspect ratios. Using the spheroid model, given in Eq. (6), a cuboid of any aspect ratio can be approximated as a spheroid by superimposing the diffusive limit of the cuboid along with a convective model, based on the ratio of the maximum perimeter of the body perpendicular to the flow direction and the square root of the total surface area. In the case of the cuboid this ratio is given as

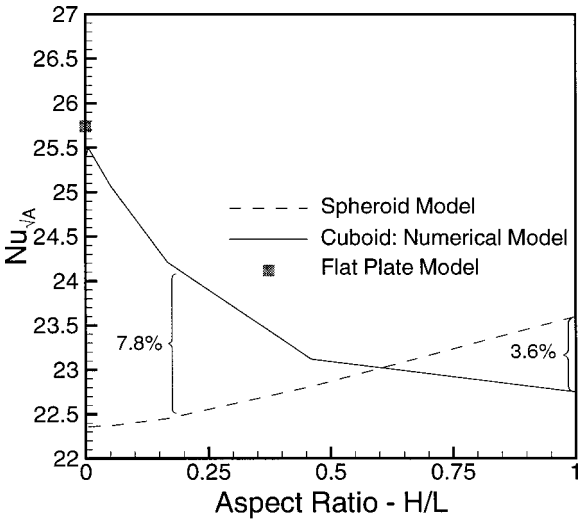

Fig. 6 Heat transfer results using the spheroid model for $0 \leqslant AR \leqslant 1$ and $Re_{\sqrt{A}}=1000$

$$\frac{P}{\sqrt{A}} = \frac{2(H+W)}{\sqrt{2(H\cdot L+H\cdot W+L\cdot W)}} \tag{25}$$

Results obtained using the spheroid model given in Eq. (6) for Reynolds number of 1000 are compared to numerical simulations using a finite volume model as shown in Fig. 6. The numerical results exhibit the correct trends with the simulation of the plate ($AR=0$) having the highest value of Nusselt number and the rate of heat transfer decreasing as the relative percentage of the surface area on the front and rear surfaces of the cuboid increases. The flat plate model of Yovanovich and Teertstra [19] is in excellent agreement with the numerical results for the flat plate, with the flat plate model being 1.4 percent higher than the numerical results. The equivalent spheroid model shows reasonable agreement for aspect ratios greater that 0.5, with a maximum difference over this range of 3.6 percent at $AR=1$. However, the inability of the equivalent spheroid model to map the correct trends with changing aspect ratio leads to a difference of greater than 12 percent at low aspect ratios. The equivalent spheroid model can be used for quick, approximate (± 3.6 percent) simulation of cuboids with aspect ratios greater that 0.33 but is not recommended as a general model for all cuboids, of arbitrary aspect ratio.

The cuboid convection model given in Eq. (19) is combined with the diffusive limit of the cuboid using Eq. (1), where a blending parameter of $n=1.3$ provides the best agreement for the full range of Reynolds number examined. While the blending parameter, n and the boundary layer parameter, $C=2.5$ have been optimized for this particular study based on comparison of model results with numerical data, it should be noted that varying these parameters over practical ranges i.e., $1 \leqslant n \leqslant 1.5$ and $2.13 \leqslant C \leqslant 2.77$ can result in changes of Nusselt numbers of ± 10 percent most notably at intermediate values of Reynolds number midway between the two defining asymptotic limits.

Table 4 Comparison of Nusselt number for the cuboid and numerical models

H/L \ $Re_{\sqrt{A}}$	0 ($S^*_{\sqrt{A}}$)		10		100		1000		5000	
	Num.	Cuboid	Num.	Cuboid	Num.	Cuboid	Num.	Cuboid	Num.	Cuboid
1.0	3.41	3.44	4.94	4.86	9.66	9.10	22.75	23.78	52.50	51.00
0.46	3.42	3.41	4.96	4.91	9.63	9.38	23.12	24.78	51.94	53.31
0.167	3.41	3.37	4.97	4.92	9.74	9.50	24.21	25.25	52.51	54.39
0.0	3.23	3.20	4.85	4.78	9.47	9.41	25.37	25.28	54.10	54.59

Table 5 Comparison of Nusselt number for the equivalent flat plate and numerical models

H/L \ $\mathrm{Re}_{\sqrt{A}}$	10			100			1000			5000		
	Num.	LB	UB	Num.	LB	UB	Num.	LB	UB	Num.	LB	UB
1.0	4.94	4.86	5.14	9.66	9.10	10.12	22.75	23.79	27.18	52.50	51.03	58.69
0.46	4.96	4.92	5.02	9.63	9.38	9.75	23.12	24.80	26.03	51.94	53.33	56.12
0.167	4.97	4.92	4.94	9.74	9.50	9.57	24.21	25.26	25.50	52.51	54.42	54.96
0.0	4.85	4.78	4.78	9.47	9.41	9.41	25.37	25.29	25.29	54.10	54.62	54.62

Table 4 presents a comparison of cuboid model results versus numerical data for a range of Reynolds number between 0 and 5000. The model results at $\mathrm{Re}_{\sqrt{A}}=0$ are the diffusive limit for the cuboid as calculated using Eqs. (2)–(5). The diffusive limit model shows agreement to within ± 1 percent of numerical validation data obtained using FLOTHERM over the full range of aspect ratios examined. Each of the other entries of total Nusselt number include the diffusive limit combined with the convective Nusselt number using a blending parameter of $n=1.3$.

The cuboid model shows excellent agreement with the validation data over the full range of Reynolds number and aspect ratios with a maximum discrepancy of 6 percent. The agreement between the model and the numerical validation data is less than 1.5 percent for the plate ($AR=0$). The improved agreement at low aspect ratio cuboids can primarily be attributed to the added confidence in the numerical data for low profile bodies.

The equivalent flat plate model provides a convenient method for approximating laminar, flow over a cuboid. The solution for Nusselt number given in Eq. (24) is dependent on fluid properties, the approach velocity and a geometric parameter that is a ratio of the flow length of the plate and the square root of the total surface area. In equating the cuboid to an equivalent flat plate, two scenarios are available for establishing the dimensions of the plate that provide an upper and lower bound on Nusselt number. The two bounding solutions are identical at an aspect ratio of zero as $H\rightarrow 0$ and the flow path length, L_p, is equivalent to the side length of the cuboid, L, for both the upper and lower bound solutions. However, as the cuboid dimensions approach the cube ($AR=1$) a minimum flow length of $L_p=2L$ is obtained for the upper bound on the Nusselt number while a maximum flow length of $L_p=(1+\sqrt{2})L$ is obtained for the lower bound on Nusselt number. Given the dependence of the Nusselt number on $L_p^{-1/2}$ the 25 percent difference in the flow length results in a difference between the upper and lower bounds on the Nusselt of approximately 15 percent for the cube.

Table 5 presents a comparison of the Nusselt number calculated using the equivalent flat plate model versus numerical data over a range of Reynolds number and aspect ratio. The equivalent flat plate model is used to calculate a lower bound (LB) and upper bound (UB) on Nusselt using the plate dimensions given in Table 2. It is interesting to note, that although the cuboid model and the equivalent flat plate model are very different in their development a near identical result is obtained with the two models when the minimum path length of $L+H$ is used as the flow length. The leading constant in both Eqs. (19) and (24) differs by less than 0.05 percent over the full range of aspect ratios examined in this study.

Conclusions

A cuboid model is presented that provides a simple, accurate method for calculating the average Nusselt number for laminar, forced convection heat transfer from isothermal cuboids of various aspect ratios. In addition, two limiting case models are presented for high and low aspect ratio bodies, i.e., the equivalent spheroid model for $AR\rightarrow 1$ and the equivalent flat plate model for $AR\rightarrow 0$. All three models are based on a blending of two asymptotic solutions, as shown in Eq. (1), namely the diffusive limit or the conduction shape factor of the cuboid given in Eq. (4) and the Nusselt number for boundary layer forced convection (spheroid model, Eq. (6), equivalent flat plate model, Eq. (24) and the cuboid model, Eq. (19)). A blending parameter of $n=1.3$ was found to provide the best agreement between the models and numerical validation results over the full range of flow conditions and geometric constraints.

The spheroid model exhibits limitations as the aspect ratio approaches zero and should be used with caution for aspect ratios less than 0.33. Both the cuboid model and the equivalent flat plate model show excellent agreement with validation data, with a maximum difference of 6 percent over the full range of Reynolds number and aspect ratios examined.

Acknowledgments

The authors would like to acknowledge the financial support of Materials and Manufacturing Ontario (MMO) and Nortel Networks Ltd., Kanata.

Nomenclature

A = surface area of the body, m^2
AR = aspect ratio, $\equiv H/L$
C = boundary layer parameter, $\equiv U_\infty/u_e$
D_{GM} = mean diameter of inscribed and circumscribed circles, m
$F(\mathrm{Pr})$ = Prandtl number function
H = cuboid height, m
k = thermal conductivity, W/(m·K)
L = cuboid length (flow direction), m
L_p = flow path length, m
L_1, L_2, L_3 = general cube dimensions, m
q = heat flux, W/m^2
n = blending parameter
Nu = Nusselt number
P = perimeter perpendicular to bulk flow, m
Pr = Prandtl number
Re = Reynolds number
S^* = dimensionless shape factor
t_e = effective residence time, s
T = temperature, °C
T_∞ = free stream temperature, °C
u_e = effective velocity, m/s
U_∞ = free stream velocity, m/s
W = cuboid width, m
x = distance in flow direction, m
x, y, z = Cartesian coordinates
X, Y, Z = domain dimensions in numerical model, m

Subscripts

$\sqrt{A}$ = characteristic length based on square root of area
bl = boundary layer
e = effective
max = maximum
min = minimum
plate = flat plate solution
s = surface

Greek Symbols

α = thermal diffusivity, m^2/s

Symbols

$\mathcal{L}$ = general characteristic length, m

References

[1] Beg, S. A., 1975, ''Forced Convection Mass Transfer Studies from Spheroids,'' Wärme - und Stoffübertragung, **8**, pp. 127–135.

[2] Refai-Ahmed, G., and Yovanovich, M. M., 1997, ''Experimental Study of Forced Convection From Isothermal Circular and Square Cylinders and Toroids,'' ASME J. Heat Transfer, **119**, pp. 70–79.

[3] Wedekind, G. L., and Kobus, C. J., 1996, ''Predicting the Average Heat Transfer Coefficient for an Isothermal Vertical Circular Disk With Assisting and Opposing Combined Forced and Natural Convection,'' Int. J. Heat Mass Transf., **39**, No. 13, pp. 2843–2845.

[4] Yovanovich, M. M., and Vanoverbeke, C. A., 1988, ''Combined Natural and Forced Convection Heat Transfer from Isothermal Spheres,'' Paper No. 88-2618, *AIAA Thermophysics, Plasmadynamics and Lasers Conference*, San Antonio, TX, June 27–29.

[5] Igarashi, T., 1985, ''Heat Transfer from a Square Prism to an Airstream,'' Int. J. Heat Mass Transf., **28**, No. 1, pp. 175–181.

[6] Igarashi, T., 1986, ''Local Heat Transfer from a Square Prism to an Airstream,'' Int. J. Heat Mass Transf., **29**, No. 5, pp. 774–784.

[7] Wong, K. L., and Chen, C. K., 1986, ''Finite Element Solutions for Laminar Flow and Heat Transfer Around a Square Prism,'' Journal of the Chinese Institute of Engineers , **9**, No. 6, pp. 605–615.

[8] Yovanovich, M. M., 1988, ''General Expression for Forced Convection Heat and Mass Transfer From Isopotential Spheroids,'' Paper No. 88-0743, *AIAA 26th Aerospace Sciences Meeting*, Reno, NV, Jan. 11–14, pp. 1–7.

[9] Wang, C.-S., Yovanovich, M. M., and Culham, J. R., 1999, ''Modeling Natural Convection From Horizontal Isothermal Annular Heat Sinks,'' ASME J. Electron. Packag., **121**, No. 1, pp. 44–49.

[10] Lee, S., Yovanovich, M. M., and Jafarpur, K., 1990, ''Effects of Geometry and Orientation on Laminar Natural Convection from Isothermal Bodies,'' AIAA J. Thermophys., **5**, No. 2, pp. 208–216.

[11] Churchill, S. W., and Usagi, R., 1972, ''A General Expression for the Correlation of Rates of Transfer and Other Phenomena,'' AIChE J., **19**, pp. 1121–1128.

[12] Rohsenow, W. M., Hartnett, J. P., and Cho, Y. I., 1998, *Handbook or Heat Transfer*, Chap. 3, McGraw-Hill, New York.

[13] Smythe, W. R., 1956, ''Charged Right Circular Cylinder,'' J. Appl. Phys., **27**, No. 8, pp. 917–920.

[14] Smythe, W. R., 1962, ''Charged Right Circular Cylinder,'' J. Appl. Phys., **33**, No. 10, pp. 2966–2967.

[15] Yuge, T., 1960, ''Experiments on Heat Transfer from Spheres Including Combined Natural and Forced Convection,'' ASME J. Heat Transfer, **82**, pp. 214–220.

[16] Yovanovich, M. M., Lee, S., and Gayowsky, T. J., 1992, ''Approximate Analytic Solution for Laminar Forced Convection From an Isothermal Plate,'' Paper No. 92-0248, *AIAA 30th Aerospace Sciences Meeting and Exhibit*, Reno, NV, Jan. 6–9.

[17] Schlichting, H., 1979, *Boundary-Layer Theory*, McGraw-Hill, Toronto.

[18] Pohlhausen, K., 1921, ''Zur näherungsweisen Integration der Differentialgleichung der laminaren Grenzschicht,'' ZAMM, **1**, pp. 252–268.

[19] Yovanovich, M. M., and Teertstra, P., 1998, ''Laminar Forced Convection From Isothermal Rectangular Plates From Small to Large Reynolds Numbers,'' Paper No. 98-2675, *7th AIAA/ASME Joint Thermophysics and Heat Transfer Conference*, Albuquerque, NM, June 15–18.

[20] FLOTHERM, 1999, Flomerics Inc., 2 Mount Royal Ave., Marlborough, MA

[21] Yovanovich, M. M., Teertstra, P., and Culham, J. R., 1995, ''Modeling Transient Conduction from Isothermal Convex Bodies of Arbitrary Shape,'' AIAA Journal of Thermophysics and Heat Transfer, **9**, No. 3, pp. 385–390.